5.4.3 Force Determination Results

a) Frequency Response Function Method

Once again the 'raw' frequency response functions were used in the analysis. The coherence function, $\gamma^2(\omega)$, associated with each frequency response function can be used to determine the random error in that measurement. The absolute error, $E(\omega)$, with a confidence limit of 99.7 per cent of the frequency response function magnitude is given by (Powell and Seering, 1984)

$$E(\omega) = 3\left|H(\omega)\right|\left[\frac{1-\gamma^2(\omega)}{2\,n_d\,\gamma^2(\omega)}\right]^{1/2} \tag{5.6}$$

where

n_d is the number of averages used in the measurements.

Calculating the absolute error for each frequency response function results in a matrix $[E(\omega)]$, with dimensions equal to that of the frequency response function matrix. The norm, $\varepsilon(\omega)$ of the $n \times m$ absolute error matrix can serve as a threshold value whereby any singular value smaller than this value will be set to zero. This will improve the condition of the problem, as the inverse of a small number is very large and would, falsely, dominate the pseudo-inverse. The singular values of the frequency response function matrix and the error norm are shown in a logarithmic plot versus frequency in the upper part of Figure 5.25. The lower part of the figure shows the anticipated trend of the condition number of $[H(\omega)]$.

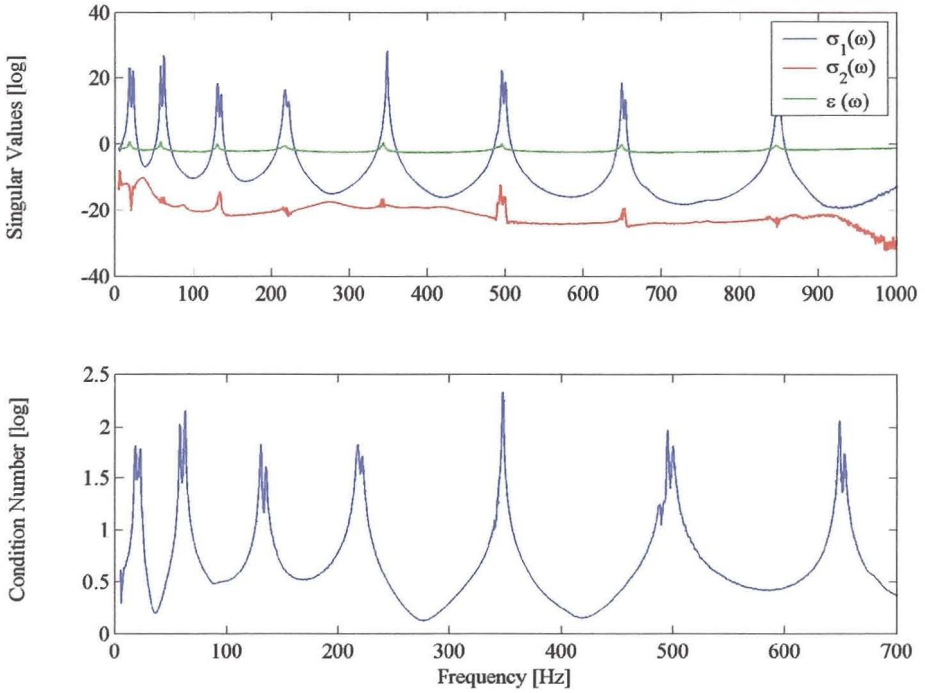

Figure 5.25– Singular values, error norm and condition number of the frequency response matrix for the hinged-hinged beam

The forces may be reconstituted from all nine sensor locations from:

$$\{\hat{F}(\omega)\} = [A(\omega)]^{+}\{\ddot{X}(\omega)\} \tag{5.7}$$

It is obvious from the results (Figure 5.26 and 527) that the frequency response function method accurately identified the two harmonic forces acting on the hinged-hinged beam.

Improving the number of response measurements will likely improve the quality of the force estimates.

The FEN for each force estimate is listed in Table 5.2

Table 5.2 - Force Error Norm of the estimated forces

$\lvert F_a(\omega)\rvert$ [%]	$\lvert F_b(\omega)\rvert$ [%]
5.291	4.724

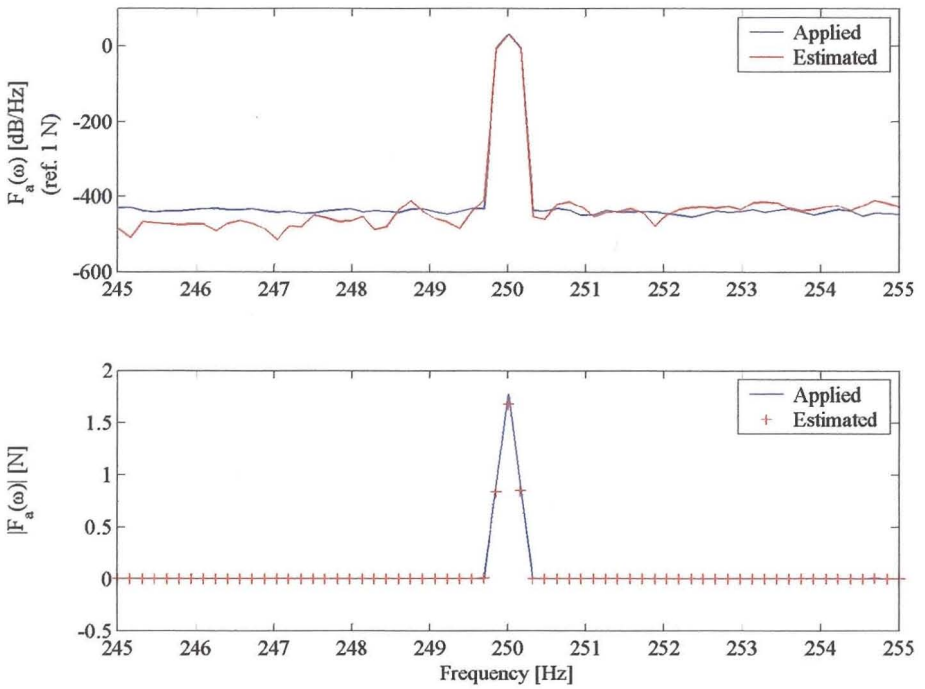

Figure 5.26 – Comparison of the measured and estimated forces applied at position 8 for the hinged-hinged beam

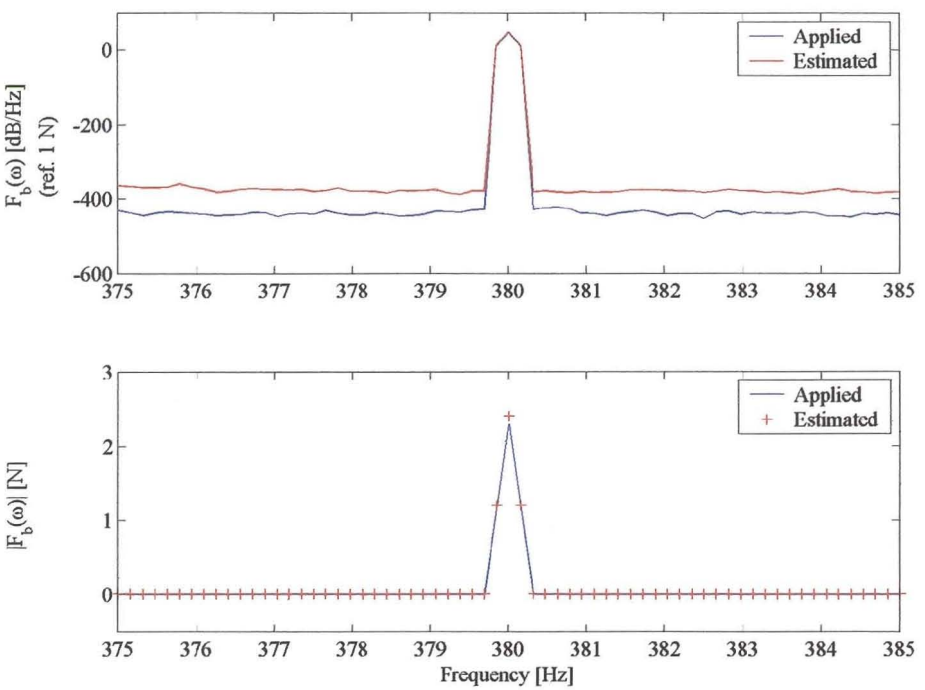

Figure 5.27 – Comparison of the measured and estimated forces applied at position 5 for the hinged-hinged beam

b) Modal Coordinate Transformation Method

The modal coordinate transformation method failed to determine the force estimates correctly.

As mentioned previously, the boundary conditions imposed on the beam were assumed to be representative of a system under operating conditions. An experimental modal analysis was performed on the measured frequency response function data in the chosen frequency range of 0-450 Hz, to extract the natural frequencies and modal damping factors corresponding to the first five bending modes. The reconstructed frequency response functions, without the contribution of the residual terms, were compared to the measured frequency response functions, prior to applying equation (4.13), from which one could determine the forces. This revealed that the residual terms had a significant effect on the accuracy of the frequency response functions in the vicinity of the forcing frequencies (250 and 380 Hz). At first, it was believed that extending the chosen frequency range to 1 kHz to include more modes could circumvent the residual contributions. Having repeated the measurements the reconstructed frequency response functions were compared with the originally measured data. The inclusion of additional modes did not improve the quality of the reconstructed frequency response functions around the fifth mode.

It is obvious from the point inertance of reference position 5, shown in Figure 5.22, that the boundary conditions influenced the proper excitation of the fifth mode (± 340 Hz). This may be attributed to a number of reasons:

Even though the mass of the concrete-filled blocks was considerably higher than that of the test piece, the question may arise whether the blocks were sufficiently rigid to provide the necessary grounding to the structure, since they had not been fixed to the floor.

Another factor that influenced the data was the supports used to constrain the beam. Tightening the bolts too much introduced spurious modes in the frequency range. Figure 5.28 illustrates the different construction methods of the supports, while Figure 5.29 demonstrates their influence on a typical frequency response function measurement. Construction method A was found to have the minimum effect on the data and was employed in the force identification process. Method B was considered not rigid enough, while C and D (attachment of G clamp) shows attempts to make the supports more rigid.

From the above, it is evident that the boundary conditions contributed to the frequency response functions of the beam. These frequency response functions were found to be too complex and could not be reconstructed from the modal parameters within the frequency range alone. Especially the frequency response functions corresponding to reference position 5 were most heavily influenced.

From the above discussion, one might suspect that better force determination will result from excluding the sensor locations, for which the reconstructed frequency response functions deviated substantially from the measured values. However, by excluding these sensor locations it was found that the condition number of the modal matrix increased significantly and also rendered inaccurate force estimates.

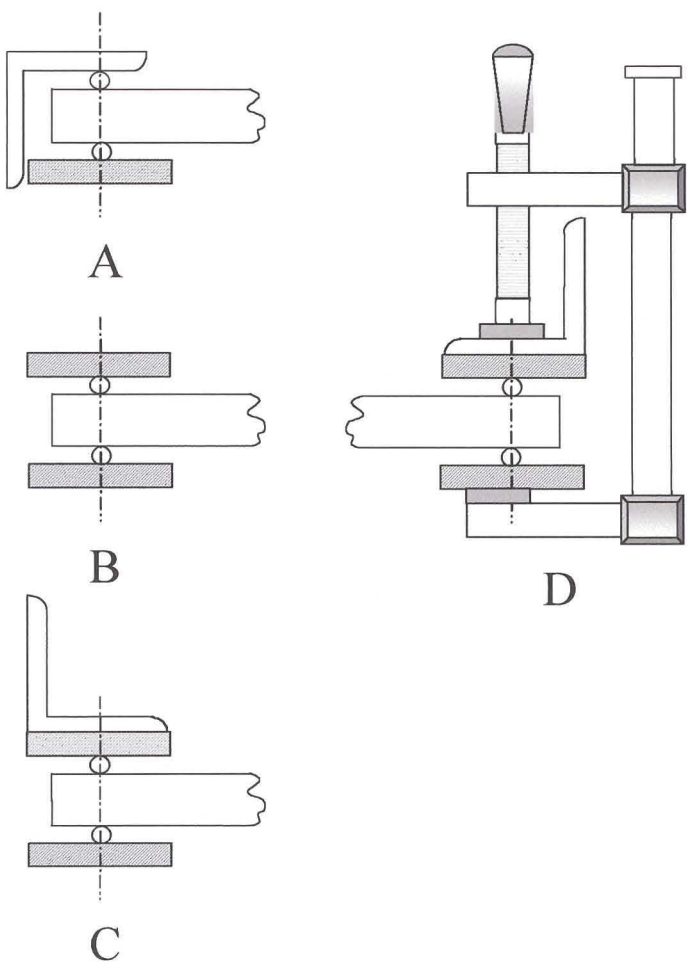

Figure 5.28 – Different constructions methods of the supports used for hinged-hinged beam

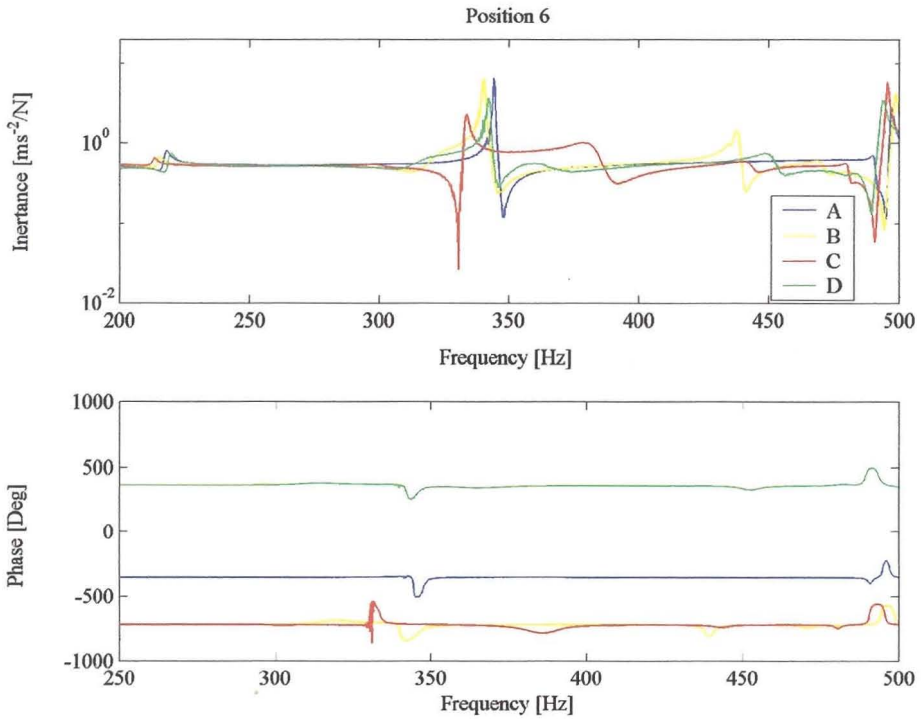

Figure 5.29 – Effect of different supports on FRF measurements corresponding to reference position 8

5.4.4 Strain Measurements

Still using the hinged-hinged beam as test piece, piezoelectric strain gauges were employed to measure frequency response functions for nine different positions along the length of the beam.

Hillary and Ewins, (1984) indicated that the strain responses gave more accurate force estimates than the accelerations. The reason for this behaviour is that the strain responses are more influenced by the higher modes at low frequencies, and therefore the frequency response functions are more complex in shape and hence obtain better force predictions. Han and Wicks (1990) also studied the application of strain measurements.

The piezoelectric strain gauges were calibrated based on the manufacturer's quoted sensitivities and the calibration values are listed in Appendix A. Only two strain gauges could be simultaneously mounted on the beam due to the restriction imposed by the available channels of the measurement system.

The Strain Frequency Response Functions (SFRFs) were measured first by taking 200 averages. Figure 5.30 and 5.31 show the SFRFs associated with each reference

position. The high level of averaging was to reduce the uncorrelated noise between the force and strain response.

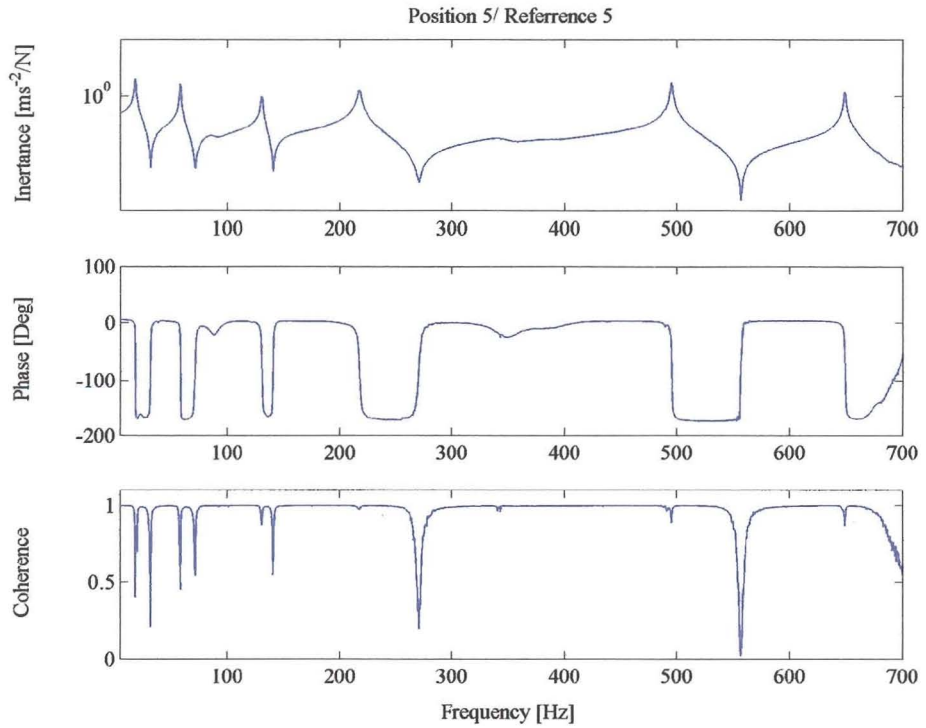

Figure 5.30 – Measured SFRF for the hinged-hinged beam corresponding to reference position 5

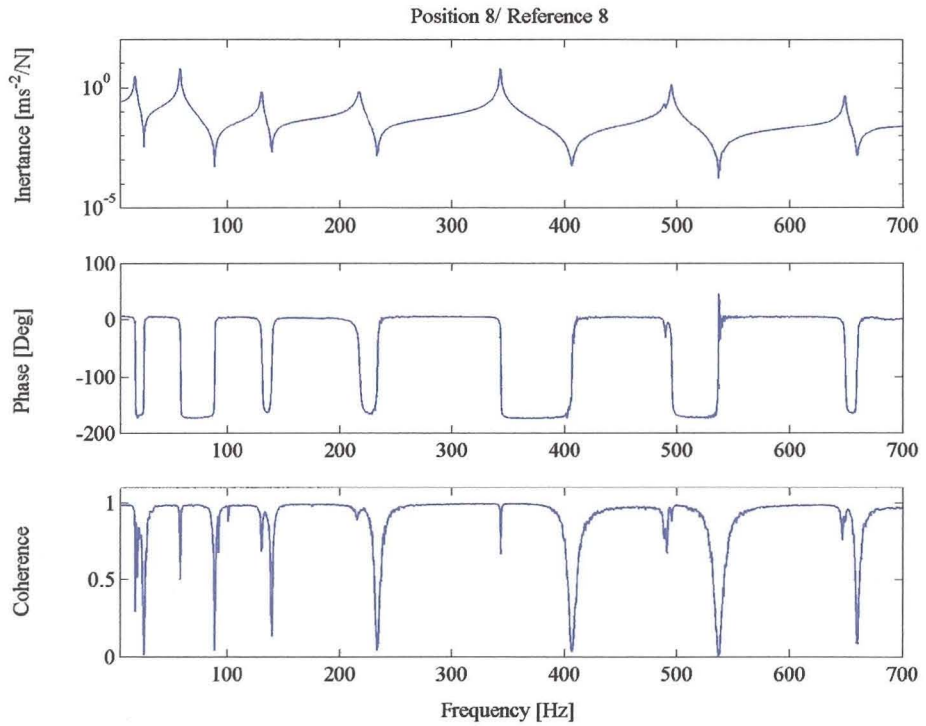

Figure 5.31 – Measured SFRF for the hinged-hinged beam corresponding to reference position 8

Subsequently, the beam was subjected to two simultaneous harmonic forces at positions 5 and 8, and strain responses were measured. An alternative formulation of equation (5.1) was used to determine the two forces.

$$\{\hat{F}(\omega)\} = [Y(\omega)]^{+}\{e(\omega)\} \tag{5.8}$$

where

$\{\hat{F}(\omega)\}$ is the (2×1) estimated force vector,

$[Y(\omega)]$ is the (2×9) SFRF matrix, and

$\{e(\omega)\}$ is the (9×1) strain response vector.

The results can be compared with the directly measured forces in Figures 5.32 and 5.33. Contrary to the expectations, it is apparent in this particular case that the acceleration responses gave better force estimates than the strain responses (Table 5.3).

Table 5.3 - Force Error Norm of the estimated forces

$\lvert F_a(\omega)\rvert$ [%]	$\lvert F_b(\omega)\rvert$ [%]
17.108	12.127

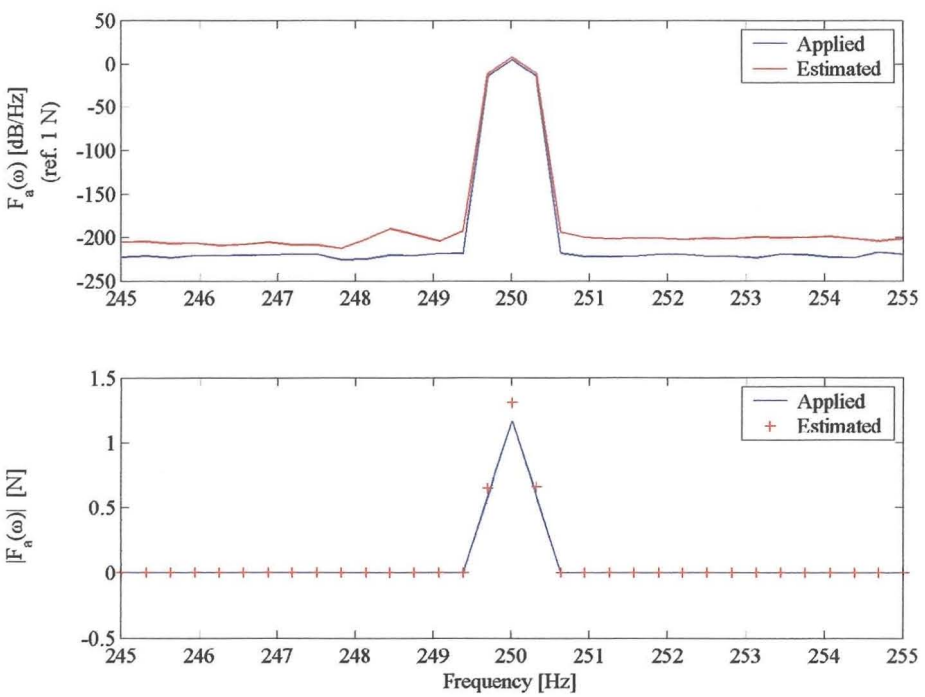

Figure 5.32 – Comparison of the measured and estimated forces applied at position 8 for the hinged-hinged beam

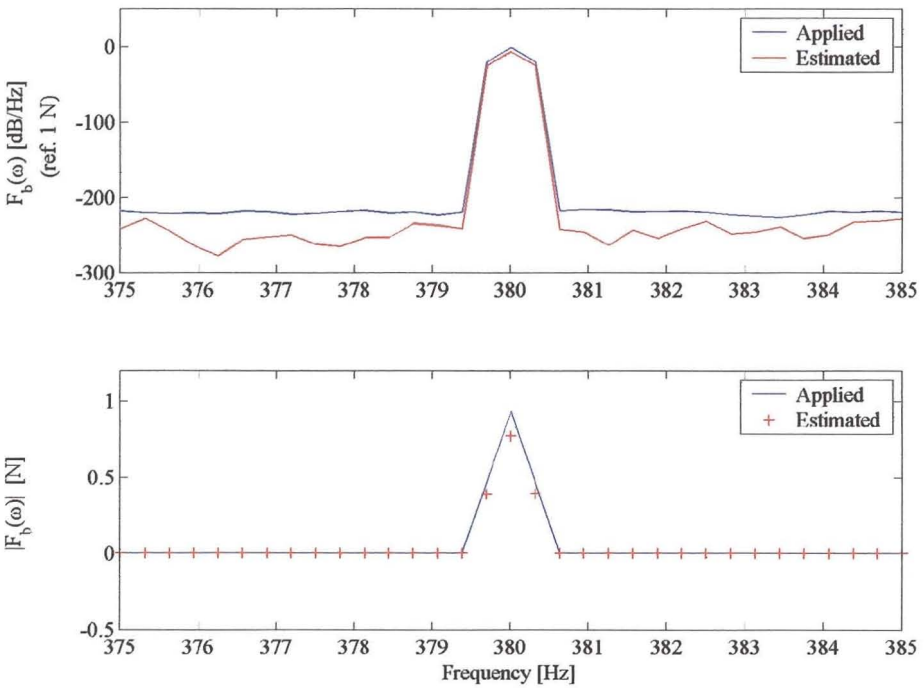

Figure 5.33 – Comparison of the measured and estimated forces applied at position 5 for the hinged-hinged beam.

As mentioned earlier, the strain response is more influenced by the higher modes at low frequencies. Conversely, the strain response is less influenced by the low modes at high frequencies. Thus, the higher the excitation frequencies the fewer modes participate in the strain response of the beam.

Having said that, the main reason for the results noted can be attributed to the sensitivity of the piezoelectric strain gauges as compared to the sensitivity of the accelerometers. Figure 5.34 shows a logarithmic plot of the singular values, the error norm of equation (5.6) and the associated condition number of the SFRF matrix. The results indicated that the values of the error norm of the SFRF matrix were higher than the corresponding values of the inertance frequency response function matrix. This parameter is employed to ascertain the random errors in the SFRF measurements and represent the probable cause for the poorer force estimates obtained. The poor coherence functions in Figure 5.29 and 5.30 confirms this statement.

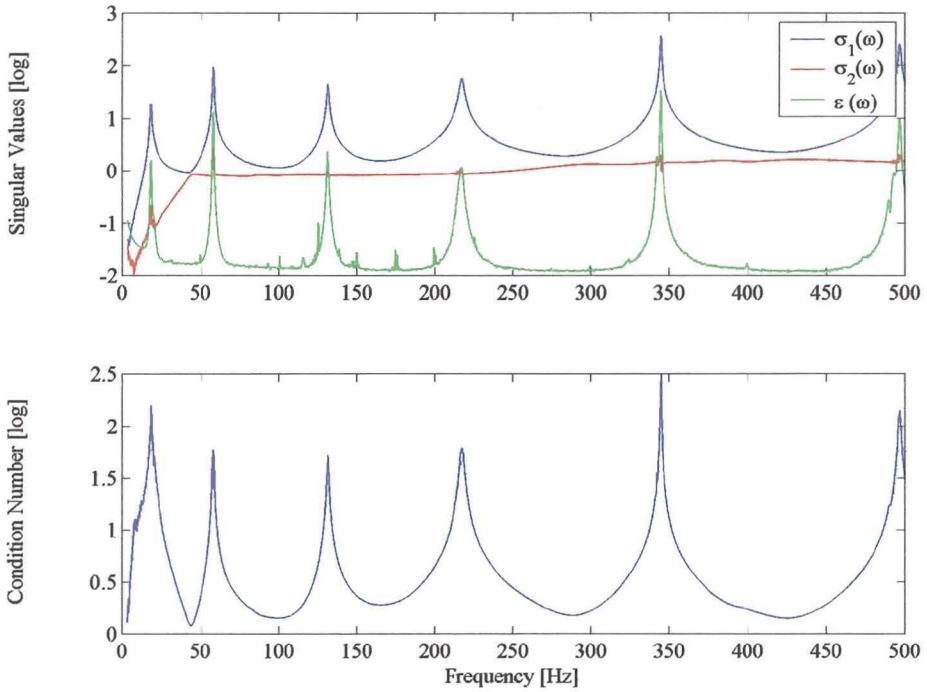

Figure 5.34 – Singular values, error norm and condition number of the SFRF matrix for the hinged-hinged beam